2000

The VSOP 5 GHz AGN Survey I. Compilation and Observations

H. Hirabayashi

E. B. Fomalont

S. Horiuchi

J. E. Lovell

G. A. Moellenbrock

See next page for additional authors

PASJ: Publ. Astron. Soc. Japan **52**, 997–1014 (2000)

The VSOP 5 GHz AGN Survey I. Compilation and Observations

Hisashi HIRABAYASHI,[1] Edward B. FOMALONT,[2] Shinji HORIUCHI,[3] James E.J. LOVELL,[4] George A. MOELLENBROCK,[5] Makoto INOUE,[3] Bernard F. BURKE,[6] Peter E. DEWDNEY,[7] Leonid I. GURVITS,[8] Hideyuki KOBAYASHI,[3] David L. JAUNCEY,[4] Yasuhiro MURATA,[1] Peter MCCULLOCH,[9] Robert A. PRESTON,[10] Ian M. AVRUCH,[1] Philip G. EDWARDS,[1] Sean M. DOUGHERTY,[7] William K. SCOTT,[11] Sandor FREY,[12] Zsolt PARAGI,[12] Yuri A. KOVALEV,[13] Misha POPOV,[13] Jonathan D. ROMNEY,[5] Richard T. SCHILIZZI,[8] Zhi-Qiang SHEN,[3] George NICOLSON,[14] Jonathan QUICK,[14] Marco COSTA,[9] Richard DODSON,[9] John E. REYNOLDS,[4] Anastasios K. TZIOUMIS,[4] Steven J. TINGAY,[4] Xiao-Yu HONG,[15] Shi-Guang LIANG,[15] Xin-Yong HUANG,[15] Wen-Ren WEI,[15] Corrado TRIGILIO,[16] Gino TUCCARI,[16] Jun'ichi NAKAJIMA,[17] Eiji KAWAI,[17] Tomofumi UMEMOTO,[3] Takeshi MIYAJI,[3] Kenta FUJISAWA,[3] Noriyuki KAWAGUCHI[3] Andrzej KUS,[18] Frank GHIGO,[19] Chris SALTER,[20] Tapasi GHOSH,[20] Boris KANEVSKY,[13] Vyacheslav SLYSH,[13] Alastair GUNN,[21] Paul BURGESS,[21] Brent CARLSON,[7] David DEL RIZZO,[7] Russell TAYLOR,[11] Wayne CANNON,[22] Seiji KAMENO,[3] Kazunori M. SHIBATA,[3] John BENSON,[13] Chris FLATTERS,[13] Andrew HALE,[13] Craig LEWIS,[13] Glen LANGSTON,[19] Anthony MINTER,[19] Kevin MILLER,[10] Joel SMITH,[10] Richard WIETFELDT,[10] Valery ALTUNIN,[10] David L. MEIER,[10] David W. MURPHY,[10] George RESCH,[10] Matthew L. LISTER,[10] B. Glenn PINER,[10] Robert JENKINS,[23] James BORDER,[24] and Jesus GIMENO[25]

[1] *The Institute of Space and Astronautical Science, Sagamihara, Kanagawa 229-8510*
[2] *National Radio Astronomy Observatory, Charlottesville, VA, USA*
[3] *National Astronomical Observatory, Mitaka, Tokyo 181-8588*
[4] *Australia Telescope National Facility, Epping, New South Wales 2122, Australia*
[5] *National Radio Astronomy Observatory, Socorro, NM 87801, USA*
[6] *Massachusetts Institute of Technology, Cambridge, MA 02139, USA*
[7] *National Research Council, Dominion Radio Astronomical Observatory, Penticton, BC, Canada*
[8] *Joint Institute for VLBI in Europe, 7991 PD Dwingeloo, The Netherlands*
[9] *University of Tasmania, Hobart, Tasmania 7000, Australia*
[10] *Jet Propulsion Laboratory, 4800 Oak Grove Drive, Pasadena, CA 91109, USA*
[11] *University of Calgary, Calgary, Alberta, T2N 1N4, Canada*
[12] *FÖMI Satellite Geodetic Observatory, H-1373 Budapest, Hungary*
[13] *Astro Space Center, P.N. Lebedev Physical Institute, Moscow 117810 GSP-1, Russia*
[14] *Hartebeesthoek Radio Astronomy Observatory, Krugersdorp 1740, South Africa*
[15] *Shanghai Astronomical Observatory, Shanghai 200030, China*
[16] *Istituto di Radioastronomia del CNR, I-96017 Noto, Italy*
[17] *Communications Research Laboratory, Kashima, Ibaraki 314-0012*
[18] *Torun Centre for Astronomy, Nicolaus Copernicus University, 87-100 Torun, Poland*
[19] *National Radio Astronomy Observatory, Green Bank, WV 24944, USA*
[20] *NAIC, Arecibo Observatory, Arecibo, 00612 Puerto Rico*
[21] *MERLIN/VLBI National Facility, Macclesfield, Cheshire SK11 9DL, UK*
[22] *CRESTech/York University, Toronto, ON M3J 1P3, Canada*
[23] *Canberra Deep Space Communications Complex, Tidbinbilla, Australia*
[24] *Goldstone Deep Space Communications Complex, Goldstone, CA, USA*
[25] *Madrid Deep Space Communications Complex, Robledo, Spain*

(Received 2000 June 30; accepted 2000 August 14)

Abstract

The VSOP mission is a Japanese-led project to image radio sources with sub-milliarcsec resolution by correlating the signal from the orbiting 8-m telescope, HALCA, with a global array of telescopes. Twenty-five percent of the scientific time of this mission is devoted to a survey of 402 bright, small-diameter extra-galactic radio sources at 5 GHz. The major goals of the VSOP Survey are statistical in nature: to determine the brightness temperature and approximate structure; to provide a source list for use with future space VLBI missions; and to compare radio properties with other data throughout the EM spectrum. This paper describes: the compilation of a complete list of radio sources associated with active galactic nuclei (AGN); the selection of the subsample of sources to be observed with VSOP; the extensive ground resources used for the Survey; the status of the observations as of 2000 July; the data-analysis methods; and several examples of results from the VSOP Survey. More detailed results from the full sample will be given in future papers.

Key word: galaxies: active — galaxies: radio — radio sources: general — techniques: interferometric

1. Introduction

On 1997 February 12 the Institute of Space and Astronautical Science (ISAS) launched an 8 m radio telescope, called HALCA, into orbit as one element of a global array of radio telescopes. This telescope is still in operation. With an apogee height of 21400 km and an orbital period of 6.3 hr, radio sources at 1.6 and 5 GHz can be imaged with a linear resolution three-times greater than with ground arrays at these frequencies (Hirabayashi et al. 1998). One of the main scientific goals of the mission is to study the radio properties of AGN at sub-milliarcsec resolution, corresponding to brightness temperatures above $\sim 10^{12}$ K.

The majority of HALCA observing time is given to peer-reviewed proposals which are solicited from the world-wide astronomical community and designated as General Observing Time (GOT) proposals. Most of these projects study the source properties by obtaining high-quality images, often at several epochs separated by days to years. However, with a detection sensitivity of ~ 0.1 Jy, hundreds of radio sources, many of which are not in the GOT proposals, can be detected with HALCA to provide a systematic study of a large sample of sources. This project was undertaken by the mission, and it is named the VSOP Survey Program.

This paper is organized as follows: (1) the compilation of the all-sky 5 GHz sample; (2) the selection of survey sources observed with HALCA; (3) the listing of the ground resources used for the survey; (4) a description of a typical experiment and the observational progress to date; (5) a brief discussion of the data-reduction techniques; and (6) typical results from an analysis of the sample. This paper is an extension that Fomalont et al. (2000a) and includes items discussed in Moellenbrock et al. (2000) and Lovell et al. (2000).

2. The VSOP All-Sky 5 GHz Flat-Spectrum Sample

The VSOP Survey sample was defined to include all cataloged extra-galactic radio sources in the sky with:

- a total cataloged flux density at 5 GHz $S_5 > 0.95$ Jy
- a spectral index $\alpha > -0.45$ (where $S \propto \nu^{\alpha}$)
- a galactic latitude $|b| > 10°$.

Our aim was to design a relatively bias-free sample to be used for statistical analyses. The source list also includes *all* extra-galactic sources with $S_5 > 5$ Jy, regardless of their spectral index and galactic latitude. Of these 37 bright sources, 21 have $\alpha < -0.5$ or $|b| < 10°$.

The existing surveys from which the 5 GHz sample were compiled were the Green Bank GB6 Catalog (Gregory et al. 1996) and the Parkes-MIT-NRAO (PMN) Survey (Lawrence et al. 1986; Griffith, Wright 1993). These surveys were conducted with several large telescopes and covered most of the sky to a flux-density level of < 0.3 Jy. Spectral information was determined from the above-mentioned catalogs or from other, more recent observations, as needed. The NASA/IPAC Extra-galactic Database (NED; http://nedwww.ipac.ca.tech.edu) provided the most convenient location for additional information. Additional sources were found in the S5 survey (Kühr et al. 1981), and from the VLBA calibrator list (http://magnolia.nrao.edu/vlba_calib/).

Since the survey observations used to compile the VSOP sample spanned a period between 1985 and 1996, source variability clearly affected the source membership in the sample. The only way to avoid such ambiguities would be to observe approximately the brightest 1000 sources in the sky at several frequencies within a short period of time; however, this effort was not possible. A source was included in the sample if the flux density at 5 GHz for *any* of the existing catalogs was > 0.95 Jy, and

there was an indication from other observations of a flat radio spectrum component within the source.

The VSOP 5 GHz flat-spectrum source list is given in table 1. It contains 402 sources and comprises about 60% of all sources above 1 Jy (Kühr et al. 1981). Previous descriptions of the VSOP Survey source list contained more than 402 sources (Fomalont et al. 2000a), but a few sources were later found to be galactic and were dropped from the list. The original plan for the VSOP Survey was to observe all sources at 5 GHz, the highest frequency and resolution of VSOP. If time permitted, an additional observation at 5 GHz or one at 1.6 GHz would be considered.

Table 1 is arranged as follows: Columns (1) and (2) give the J2000 source name and the common source name. An asterisk (*) after the J2000 name indicates that the spectral index or galactic latitude are outside of the sample specifications and the source is not formally part of the complete sample. Some of these sources have $S_5 > 5.0$ Jy (all such sources were included) and some sources appear to have a spectral index $\alpha < -0.45$, based on information not available when the source list was first compiled. Columns (3) and (4) give the source coordinates at epoch J2000. The accuracy of the position is implied by the number of significant digits and generally refers to the peak position of the brightest component in a complex source. For a majority of the sources, milliarcsecond–accurate positions were available from the US Naval Observatory (USNO) catalog of the International Celestial Reference Frame source (Johnston et al. 1995) or from the VLA and the VLBA source list, compiled by NRAO. The next three columns list the galactic latitude (b), the total flux density at 5 GHz (S_5) derived from the catalogs, and the spectral index (α). As described above, the flux density and spectral index of many of the sources vary significantly over periods of more than about one year. The last three columns are associated with VLBA observations (Fomalont et al. 2000b) which are described in the next section.

3. The Survey Sources Observed with VSOP

In order to maximize the return from the HALCA observations, those sources with a known low correlated flux density at 5 GHz on the largest earth baselines were not included in the source list to be observed by HALCA. These sources would be very weak or resolved with space baselines, and nearly all would be difficult to detect.

This selection was accomplished in large part in 1996 June by 22 hr of observations with the VLBA at 5 GHz for all sources in table 1 which were north of declination $-44°$, plus a few additional sources which were not greater than 1 Jy in the finding catalogs, but appeared to be stronger in 1996. Although each source was observed for only 150 s, accurate correlated flux densities and good-quality images with 2 milli-arcsecopnd (mas) resolution were obtained. A detailed presentation of these observations and the resulting 5 GHz VLBI catalog, the VLBApls Catalog, are given elsewhere (Fomalont et al. 2000b).

The pertinent information from the VLBApls catalog for source inclusion as a HALCA target is shown in the last three columns of table 1: (1) S_{2M} : the correlated flux density at 5 GHz at 2×10^6 wavelengths (2 Mλ); (2) S_{140M} : the correlated flux density at 140×10^6 wavelengths (140 Mλ); and (3) the code used for the VSOP Survey observation. The correlated flux density at 140 Mλ was used as the criterion for inclusion of the source in the HALCA observing list. Since the detection level for typical HALCA survey observations is ~ 0.1 Jy, a correlated flux density of $S_{140M} < 0.3$ Jy precluded detection on space baselines which are as long as 500 Mλ at 5 GHz. Those sources above this limit were given a VSOP observation code. The observation codes begin with vs01a for the strongest source (J1230+1223) and end with vs12c for the weakest (J0205+3212), according to S_5 in table 1. The correlated flux density at the shortest VLBA spacing, S_{2M}, was occasionally larger than the total flux density from the finding catalogs, and this higher value was assigned to S_5.

Additional information on the milli-arcsecond structure for the survey radio sources was obtained from: the VLBA calibrator list (Peck, Beasley 1998); the USNO geodetic catalog and the International Celestial Reference Frame (ICRF) information (http://maia.usno.navy.mil/rorf/rrfid.html); the 15 GHz VLBA survey (Kellermann et al. 1998); trans-continental surveys at 2.29 GHz (Preston et al. 1985) and 22 GHz (Moellenbrock et al. 1996); and from southern hemisphere VLBI observations (Tingay et al. in preparation)

From these VLBI ground observations, 113 of the 402 sources in the VSOP all-sky 5 GHz flat-spectrum sample were found to be sufficiently resolved on ground baselines, and probably not detectable with VSOP observations. The remaining 289 sources are the survey sources that will be observed with HALCA, and are indicated with a VSOP observation code. Although observations are being made only for this sub-sample, all 402 sources in the complete sample should be included in any statistical studies of these AGN. We will designate this sample of 289 source as the VSOP Source Sample (VSS).

After six months of VSOP observations it was apparent that the time needed for HALCA to slew between sources and recalibrate the drift rates of the gyroscopes was longer than expected, decreasing the number of targets that could be observed. Thus, for those 5 GHz GOT observations of sources in the VSS, permission was requested from the relevant principal investigators (PIs) to extract a limited part of their observations for the use in the Survey Program, but only for statistical purposes.

Table 1. The VSOP 5 GHz AGN survey source list

Source name J2000	Source name Common	R.A. J2000	Declination J2000	b (°)	S_5 (Jy)	α	S_{2M} (Jy)	S_{140M} (Jy)	Observation code
J0006−0623	0003−066	00 06 13.8928	−06 23 35.334	−66.6	2.5	0.9	2.40	1.20	vs03t
J0013+4051	0010+405	00 13 31.1301	+40 51 37.144	−21.4	1.0	0.0	0.56	0.24	
J0019+7327	0016+731	00 19 45.7863	+73 27 30.017	10.7	1.7	−0.4	1.28	0.96	vs07a
J0029+3456	0025+345	00 29 14.2426	+34 56 32.247	−27.7	1.3	0.0	1.12	< 0.10	
J0038+4137	0035+413	00 38 24.8436	+41 37 06.000	−21.2	1.1	0.0	0.56	< 0.10	
J0042+2320	0039+230	00 42 04.5451	+23 20 01.061	−39.5	1.6	1.0	0.96	0.32	vs07u
J0050−0929*	0048−097	00 50 41.3173	−09 29 05.209	−72.4	1.9	−0.7	1.20	1.20	vs06i
J0059+0006*	0056−001	00 59 05.5149	+00 06 51.622	−62.7	1.4	−0.6	0.96	0.16	
J0105+4819	0102+480	01 05 49.9295	+48 19 03.182	−14.5	1.1	0.0	1.12	0.64	vs08q
J0106−4034	0104−408	01 06 45.1079	−40 34 19.959	−76.2	2.6	2.6	2.40	1.60	vs03s
J0108+0135	0106+013	01 08 38.7710	+01 35 00.317	−61.0	3.4	1.3	1.60	0.40	vs02t
J0111+3906	0108+388	01 11 37.3167	+39 06 28.103	−23.6	1.3	0.0	1.28	0.16	
J0115−0127	0112−017	01 15 17.0999	−01 27 04.576	−63.7	1.6	0.8	1.12	0.40	vs07t
J0116−1136	0113−118	01 16 12.5219	−11 36 15.432	−73.4	1.9	−0.3	1.12	0.48	vs06h
J0119+0829	0116+082	01 19 01.274	+08 29 54.68	−53.8	1.2	0.0	0.48	< 0.10	
J0119+3210	0116+319	01 19 35.0001	+32 10 50.058	−30.3	1.6	−0.4	0.72	< 0.10	
J0120−2701	0118−272	01 20 31.6634	−27 01 24.651	−83.5	1.2	0.1	0.80	0.24	
J0121+1149	0119+115	01 21 41.5950	+11 49 50.413	−50.4	1.1	0.0	1.12	1.12	vs08p
J0121+0422	0119+041	01 21 56.8616	+04 22 24.734	−57.6	2.0	0.0	1.36	0.80	vs05y
J0125−0005	0122−003	01 25 28.8427	−00 05 55.963	−61.8	1.6	0.1	1.60	0.40	vs05x
J0126−0123	0123−016	01 26 03.10	−01 23 26.1	−63.0	1.3	0.2	< 0.10	< 0.10	
J0126+2559	0123+257	01 26 42.7926	+25 59 01.301	−36.2	1.4	0.0	0.80	0.80	vs08o
J0132−1654	0130−171	01 32 43.487	−16 54 48.51	−76.0	1.2	−0.5	1.20	0.56	vs08c
J0134−3629	0131−367	01 34 12.0	−36 29 14.0	−77.1	1.7				
J0136+4751	0133+476	01 36 58.5947	+47 51 29.100	−14.3	2.4	0.0	2.40	2.40	vs03r
J0137−2430*	0135−247	01 37 38.3463	−24 30 53.884	−79.3	1.6	−0.6	1.20	1.04	vs07s
J0137+3309*	3C 48	01 37 41.2994	+33 09 35.134	−28.7	5.8	−0.8	0.56	< 0.10	
J0141−0928	0138−097	01 41 25.8320	−09 28 43.673	−68.8	1.2	0.5	0.56	0.32	vs10i
J0149+0555	0146+056	01 49 22.3709	+05 55 53.568	−54.1	1.5	0.0	1.36	0.64	vs06z
J0152+2207	0149+218	01 52 18.0590	+22 07 07.700	−38.6	1.1	0.0	1.12	1.12	vs08n
J0153−3310	0150−334	01 53 10.1217	−33 10 25.861	−75.4	1.4	0.7	0.88	0.24	
J0155−4048	0153−410	01 55 37.0593	−40 48 42.358	−71.0	1.2	−0.1	0.88	0.16	
J0157+7442	0153+744	01 57 34.9648	+74 42 43.230	12.4	1.5	−0.3	1.28	< 0.10	
J0202−7620	0202−765	02 02 13.6945	−76 20 03.056	−40.0	1.0	−0.5			vs11l
J0204+1514	0202+149	02 04 50.4139	+15 14 11.043	−44.0	2.7	−0.2	2.48	2.00	vs03i
J0204−1701	0202−172	02 04 57.6743	−17 01 19.839	−70.2	1.4	−0.1	1.20	0.80	vs08b
J0205+3212	0202+319	02 05 04.9253	+32 12 30.095	−28.1	1.0	0.0	0.80	0.56	vs12c
J0210−5101	0208−512	02 10 46.2003	−51 01 01.892	−61.8	3.3	−0.2	0.40	0.40	vs03a
J0217+7349	0212+735	02 17 30.8132	+73 49 32.621	12.0	3.2	−0.1	3.20	2.16	vs02o
J0217+0144	0215+015	02 17 48.9547	+01 44 49.699	−54.4	1.6	1.4	0.96	0.88	vs07r
J0221+3556	0218+357	02 21 05.4733	+35 56 13.791	−23.5	1.5	0.0	0.88	< 0.10	
J0224+0659	0221+067	02 24 28.4281	+06 59 23.342	−49.1	1.0	0.0	0.64	0.48	vs12b
J0226+3421	0223+341	02 26 10.333	+34 21 30.29	−24.6	1.7	−0.2	1.68	0.32	vs05o
J0231+1322	0229+131	02 31 45.8940	+13 22 54.716	−42.7	2.4	1.0	1.36	0.88	vs04l
J0237+2848	0234+285	02 37 52.4056	+28 48 08.990	−28.5	3.4	0.5	2.00	1.20	vs02s
J0238+1636	0235+164	02 38 38.9301	+16 36 59.275	−39.1	1.9	0.0	0.48	0.24	
J0239+0416	0237+040	02 39 51.2630	+04 16 21.412	−49.1	1.1	0.0	0.88	0.56	vs11i
J0240−2309	0237−233	02 40 08.1745	−23 09 15.730	−65.1	3.6	0.7	2.80	0.16	
J0241−0815	NGC 1052	02 41 04.7985	−08 15 20.751	−57.9	3.2	2.9	2.48	0.16	
J0242+1101	0239+108	02 42 29.1708	+11 01 00.728	−43.3	1.6	0.0	1.60	0.80	vs05w

Table 1. (Continued.)

Source name J2000	Common	R.A. J2000	Declination J2000	b (°)	S_5 (Jy)	α	S_{2M} (Jy)	S_{140M} (Jy)	Observation code
J0251+4315	0248+430	02 51 34.5367	+43 15 15.829	−14.4	1.4	0.0	1.28	0.40	vs07q
J0253−5441	0252−549	02 53 29.1805	−54 41 51.436	−54.6	1.2	0.8			vs09o
J0259+0747	0256+075	02 59 27.0766	+07 47 39.643	−43.3	1.0	0.0	0.72	0.56	vs12a
J0303−6211	0302−623	03 03 50.6316	−62 11 25.549	−48.7	2.2	0.9			vs04v
J0309−6058	0308−611	03 09 56.0996	−60 58 39.059	−48.9	1.3	0.4			vs08u
J0312+0133	0310+013	03 12 43.603	+01 33 17.57	−45.5	1.0	0.0	0.40	0.40	vs11z
J0318+4151	NGC 1265	03 18 15.738	+41 51 27.38	−13.1	1.5	0.9	< 0.10	< 0.10	
J0319+4130	3C84	03 19 48.1601	+41 30 42.106	−13.3	42.4	0.0	24.00	1.60	vs01c
J0321+1221	0319+121	03 21 53.1034	+12 21 13.954	−36.2	1.6	0.3	1.28	0.80	vs07p
J0322−3712*	For A	03 22 41.52	−37 12 33.5	−56.7	45.0	−0.8	< 0.10	< 0.10	
J0334−4008*	0332−403	03 34 13.6544	−40 08 25.396	−54.1	2.6	−0.7	2.08	1.84	vs04b
J0336+3218	NRAO 140	03 36 30.1076	+32 18 29.342	−18.8	2.0	−0.4	1.76	0.48	vs05f
J0339−0146	CTA 26	03 39 30.9377	−01 46 35.803	−42.5	3.0	0.3	2.00	0.64	vs03q
J0348−2749	0346−279	03 48 38.144	−27 49 13.56	−50.9	1.4	0.5	1.04	0.88	vs08m
J0359+5057*	NRAO 150	03 59 29.7472	+50 57 50.162	−1.6	10.1	0.1	1.60	0.32	vs01i
J0402−3147	0400−319	04 02 21.2660	−31 47 25.945	−48.5	1.0	−0.5	0.72	0.32	vs11y
J0403+2600	0400+258	04 03 05.5860	+26 00 01.503	−19.6	1.0	0.0	0.80	0.40	vs11x
J0403−3605	0402−362	04 03 53.7499	−36 05 01.912	−48.5	2.2	1.0	2.16	2.16	vs03z
J0405−1308	0403−132	04 05 34.0033	−13 08 13.689	−42.7	3.2	−0.2	0.80	0.80	vs03e
J0406−3826	0405−385	04 06 59.0349	−38 26 28.039	−47.9	1.3	−0.4	1.28	1.20	vs07o
J0407−1211*	0405−123	04 07 48.4308	−12 11 36.658	−41.8	1.8	−1.2	0.64	0.48	vs06q
J0412+2305	0409+229	04 12 43.6667	+23 05 05.477	−20.1	1.0	0.0	0.32	< 0.10	
J0414+3418	0411+341	04 14 37.255	+34 18 51.20	−12.0	1.6	0.0	1.60	< 0.10	
J0414+0534	0411+054	04 14 37.768	+05 34 42.33	−31.0	1.1	0.0	0.24	< 0.10	
J0416−1851*	0414−189	04 16 36.5444	−18 51 08.339	−42.4	1.3	−0.7	1.20	1.04	vs08a
J0423−0120	0420−014	04 23 15.8007	−01 20 33.064	−33.1	4.4	1.2	3.04	2.00	vs02g
J0424−3756	0422−380	04 24 42.2437	−37 56 20.782	−44.4	1.7	2.1	1.20	0.64	vs06y
J0424+0036	0422+004	04 24 46.8420	+00 36 06.330	−31.8	1.5	0.0	0.48	0.40	vs07z
J0428−3756	0426−380	04 28 40.4243	−37 56 19.578	−43.6	1.8	0.2	1.76	1.44	vs05e
J0431+2037	0428+205	04 31 03.762	+20 37 34.25	−18.6	2.8	−0.1	1.68	< 0.10	
J0433+0521	3C 120	04 33 11.0955	+05 21 15.620	−27.4	3.8	−0.2	3.20	0.40	vs02n
J0437−1844	0434−188	04 37 01.4827	−18 44 48.612	−37.8	1.2	0.1	1.04	0.48	vs09m
J0437+2940*	3C 123	04 37 04.375	+29 40 13.82	−11.7	14.9	−1.1	0.16	< 0.10	
J0440−4333*	0438−436	04 40 17.1799	−43 33 08.603	−41.6	7.0	−0.9	2.00	0.96	vs01r
J0442−0017*	NRAO 190	04 42 38.6607	−00 17 43.419	−28.5	3.1	−0.9	1.52	0.48	vs03h
J0449+1121	0446+112	04 49 07.6711	+11 21 28.597	−20.7	1.0	0.0	0.96	0.48	vs10h
J0450−8101	0454−810	04 50 05.4400	−81 01 02.233	−31.4	1.4	0.3	< 0.10	0.40	vs08l
J0453−2807	0451−282	04 53 14.6468	−28 07 37.327	−37.0	2.5	−0.2	2.00	0.40	vs04g
J0455−3006	0453−301	04 55 14.31	−30 06 49.9	−37.1	1.5	−0.5	< 0.10	< 0.10	
J0457−2324	0454−234	04 57 03.1792	−23 24 52.018	−34.9	2.0	0.1	1.68	1.12	vs05n
J0459+0229	0457+024	04 59 52.0506	+02 29 31.176	−23.3	1.7	0.1	1.68	0.32	vs05m
J0501−0159	0458−020	05 01 12.8098	−01 59 14.255	−25.3	3.3	1.0	2.08	1.04	vs02z
J0503+0203	0500+019	05 03 21.1971	+02 03 04.677	−22.8	2.1	−0.5	2.08	0.64	vs04a
J0508+8432	0454+844	05 08 42.3633	+84 32 04.544	24.7	1.1	−0.2	0.40	0.40	vs11h
J0509+0541	0506+056	05 09 25.964	+05 41 35.34	−19.6	1.0	0.0	0.48	0.40	vs11w
J0513−2159*	0511−220	05 13 49.1143	−21 59 16.090	−30.8	1.3	−0.6	0.72	0.32	vs09l
J0519−4546*	Pic A	05 19 49.75	−45 46 43.8	−34.6	5.8	−1.0	0.16	0.16	
J0522−3627*	0521−365	05 22 57.9846	−36 27 30.849	−32.7	9.2	−0.7	2.40	0.80	vs01j
J0525−4557	0524−460	05 25 31.4002	−45 57 54.685	−33.7	1.9	1.2			vs06a
J0530−2503*	0528−250	05 30 07.9627	−25 03 29.898	−28.2	1.1	−0.8	0.88	0.24	

Table 1. (Continued.)

Source name J2000	Source name Common	R.A. J2000	Declination J2000	b (°)	S_5 (Jy)	α	S_{2M} (Jy)	S_{140M} (Jy)	Observation code
J0530+1331	0528+134	05 30 56.4167	+13 31 55.150	−11.0	6.2	0.0	6.24	4.24	vs01o
J0532+0732	0529+075	05 32 38.9984	+07 32 43.345	−13.7	2.0	−0.1	2.00	< 0.10	
J0538−4405	0537−441	05 38 50.3618	−44 05 08.939	−31.1	4.8	0.4	< 0.10	0.80	vs02c
J0539−2839	0537−286	05 39 54.2814	−28 39 55.946	−27.3	1.2	0.9	0.48	0.32	vs10g
J0541−0541	0539−057	05 41 38.0833	−05 41 49.427	−18.1	1.2	0.9	1.20	0.48	vs07y
J0542+4951*	3C 147	05 42 36.1378	+49 51 07.233	10.3	7.5	−1.0	2.08	0.40	vs01p
J0555+3948*	DA 193	05 55 30.8056	+39 48 49.165	7.3	6.3	0.9	6.32	3.60	vs01n
J0604−3155	0602−310	06 04 14.48	−31 55 57.9	−23.3	1.4	−0.5	< 0.10	< 0.10	
J0607+6720	0602+673	06 07 52.670	+67 20 55.41	20.9	1.0	0.0	0.80	0.80	vs11v
J0607−0834	0605−085	06 07 59.6992	−08 34 49.977	−13.5	2.4	−0.4	2.40	1.44	vs03p
J0609−1542	0607−157	06 09 40.9494	−15 42 40.671	−16.2	4.2	0.2	4.16	2.00	vs02a
J0614+6046	0609+607	06 14 23.8661	+60 46 21.755	19.1	1.1	0.0	0.96	0.72	vs10f
J0616−3456	0614−349	06 16 35.9813	−34 56 16.563	−21.8	1.4	−0.5	< 0.10	< 0.10	
J0620−3711	0618−371	06 20 00.83	−37 11 37.6	−21.9	1.4	−0.5	0.16	< 0.10	
J0626+8202	0615+820	06 26 03.0061	+82 02 25.568	26.0	1.0	−0.1	0.80	0.40	vs11u
J0627−3529	0625−354	06 27 06.728	−35 29 15.32	−20.0	2.2	−0.4	0.72	< 0.10	
J0627−0553*	3C 161	06 27 10.0960	−05 53 04.768	−8.1	7.5	−0.7	< 0.10	< 0.10	
J0635−7516	0637−752	06 35 46.5082	−75 16 16.816	−27.2	6.4	0.1	3.44	1.60	vs01t
J0636−2034	0634−205	06 36 32.67	−20 34 53.4	−12.4	1.3		< 0.10	< 0.10	
J0644−3459	0642−349	06 44 25.281	−34 59 41.93	−16.5	1.0	0.2	0.96	0.40	vs10e
J0646+4451	0642+449	06 46 32.0259	+44 51 16.590	17.9	1.7	0.0	1.68	1.52	vs05l
J0648−3957	0636−398	06 48 12.10	−39 57 02.0	−17.6	1.1	−0.5	0.16	< 0.10	
J0648−3044	0636−306	06 48 14.0964	−30 44 19.658	−14.1	1.0	−0.5	0.80	0.48	vs11t
J0713+4349	0710+439	07 13 38.1640	+43 49 17.204	22.2	1.6	−0.3	1.44	0.40	vs06p
J0714+3534	0711+356	07 14 24.8175	+35 34 39.793	19.7	1.0	0.0	1.04	0.80	vs09k
J0738+1742	0735+178	07 38 07.3937	+17 42 18.999	18.1	2.2	0.2	1.44	0.56	vs05d
J0739+0137	0736+017	07 39 18.0338	+01 37 04.619	11.4	1.8	−0.4	1.76	0.88	vs05c
J0741+3112	0738+313	07 41 10.7033	+31 12 00.229	23.6	3.4	0.2	3.36	1.60	vs02k
J0743−6726	0743−673	07 43 31.6129	−67 26 25.541	−20.1	2.2	−0.3			vs04u
J0745+1011	0742+103	07 45 33.0595	+10 11 12.693	16.6	3.5	−0.1	3.36	1.20	vs02j
J0745−0044	0743−006	07 45 54.0823	−00 44 17.538	11.7	2.0	1.1	2.00	0.96	vs04f
J0748+2400	0745+241	07 48 36.1092	+24 00 24.110	22.7	1.2	0.0	0.80	0.56	vs10d
J0750+1231	0748+126	07 50 52.0457	+12 31 04.829	18.8	1.9	0.0	1.92	1.36	vs04k
J0758+3747	NGC 2484	07 58 28.108	+37 47 11.81	28.8	1.0	0.0	0.24	< 0.10	
J0808−0751	0805−077	08 08 15.5360	−07 51 09.885	13.2	1.6	0.6	0.96	0.24	
J0808+4950	0804+499	08 08 39.6662	+49 50 36.530	32.6	1.2	0.0	1.04	0.80	vs09j
J0811+0146	0808+019	08 11 26.7073	+01 46 52.221	18.6	1.5	0.0	1.28	1.28	vs07n
J0815+3635	0812+367	08 15 25.9448	+36 35 15.148	31.9	1.0	0.0	0.96	0.96	vs10c
J0818+4222	0814+425	08 18 15.9996	+42 22 45.415	33.4	1.9	−0.1	1.12	0.40	vs06g
J0820−1258	0818−128	08 20 57.4475	−12 58 59.168	13.2	1.0	0.3	0.48	0.32	vs11s
J0823+2223	0820+225	08 23 24.760	+22 23 03.28	29.7	1.6	−0.1	1.20	0.24	
J0824+5552	0820+560	08 24 47.2363	+55 52 42.669	35.1	1.2	0.0	1.04	0.64	vs09i
J0824+3916	0821+394	08 24 55.4838	+39 16 41.904	34.2	1.0	0.0	0.96	0.96	vs10b
J0825+0309	0823+033	08 25 50.3383	+03 09 24.521	22.4	1.6	0.0	1.60	1.36	vs05v
J0831+0429	0829+046	08 31 48.8769	+04 29 39.086	24.3	2.1	2.2	1.12	0.40	vs05k
J0834+5534	0831+557	08 34 54.9040	+55 34 21.071	36.6	5.8	−0.5	4.80	0.24	
J0836−2016*	0834−201	08 36 39.2152	−20 16 59.501	12.2	2.6	−1.5	2.64	1.36	vs02y
J0840+1312	0838+133	08 40 47.589	+13 12 23.56	30.1	1.3	0.0	0.56	0.40	vs09h
J0841+7053	0836+710	08 41 24.3652	+70 53 42.173	34.4	2.4	−0.5	2.00	0.40	vs04e
J0842+1835	0839+187	08 42 05.0941	+18 35 40.991	32.5	1.0	0.0	0.96	0.32	vs10a

Table 1. (Continued.)

Source name J2000	Common	R.A. J2000	Declination J2000	b (°)	S_5 (Jy)	α	S_{2M} (Jy)	S_{140M} (Jy)	Observation code
J0854+5757	0850+581	08 54 41.9963	+57 57 29.939	38.9	1.2	0.0	0.88	0.72	vs09z
J0854+2006	OJ 287	08 54 48.8749	+20 06 30.641	35.8	2.7	−0.2	1.52	0.88	vs03y
J0900−2808	0858−279	09 00 40.039	−28 08 20.35	11.8	3.6	0.2	3.60	< 0.10	
J0903+4651	0859+470	09 03 03.9901	+46 51 04.137	41.6	1.3	0.0	0.80	0.56	vs09g
J0909+0121	0906+015	09 09 10.0916	+01 21 35.618	30.9	1.0	0.0	0.48	0.32	vs11r
J0909+4253*	0906+432	09 09 33.497	+42 53 46.48	42.8	1.5	−0.7	0.64	0.56	vs07m
J0920+4441	0917+449	09 20 58.4584	+44 41 53.985	44.8	1.2	0.0	1.20	1.04	vs07x
J0921−2618	0919−260	09 21 29.3538	−26 18 43.385	16.5	2.3	1.2	1.44	0.32	vs04s
J0921+6215	0917+624	09 21 36.2311	+62 15 52.180	41.0	1.5	0.0	1.52	1.36	vs06f
J0927+3902	4C 39.25	09 27 03.0139	+39 02 20.852	46.2	11.2	0.8	11.20	7.20	vs01f
J0948+4039	0945+408	09 48 55.3381	+40 39 44.587	50.3	1.6	0.3	1.60	1.44	vs05u
J0949+6614	0945+664	09 49 12.2100	+66 14 59.321	41.9	1.4	0.0	< 0.10	< 0.10	
J0956+2515	0953+254	09 56 49.8753	+25 15 16.050	51.0	1.3	0.0	1.28	0.48	vs07l
J0957+5522	0954+556	09 57 38.184	+55 22 57.76	47.9	2.3	−0.2	0.72	< 0.10	
J0958+4725	0955+476	09 58 19.6716	+47 25 07.842	50.7	1.3	0.0	1.28	1.28	vs07k
J0958+6533	0954+658	09 58 47.2451	+65 33 54.818	43.1	1.4	0.0	0.72	0.72	vs08k
J1006+3454	3C 236	10 06 01.750	+34 54 10.40	54.0	1.7	−0.3	0.24	< 0.10	
J1014+2301	1012+232	10 14 47.0654	+23 01 16.571	54.4	1.1	0.0	0.80	0.56	vs11g
J1018−3144	1015−314	10 18 09.269	−31 44 14.09	20.7	1.8	−0.4	0.56	< 0.10	
J1035−2011	1032−199	10 35 02.1552	−20 11 34.358	32.3	1.1	−0.1	0.64	0.40	vs11f
J1035+5628	1031+567	10 35 07.0399	+56 28 46.792	51.9	1.3	0.0	1.28	0.24	
J1037−2934	1034−293	10 37 16.0797	−29 34 02.812	24.8	1.6	0.2	1.60	1.44	vs05t
J1041+0610	1038+064	10 41 17.1625	+06 10 16.924	52.7	1.7	0.0	1.68	1.44	vs05j
J1041+0242	1039+029	10 41 38.8819	+02 42 30.816	50.5	1.1	0.0	< 0.10	< 0.10	
J1042+1203	3C 245	10 42 44.6052	+12 03 31.264	56.3	1.7	−0.3	0.80	0.24	
J1044+8054	1039+811	10 44 23.0626	+80 54 39.443	34.7	1.1	0.1	0.72	0.40	vs11e
J1048−1909	1045−188	10 48 06.6204	−19 09 35.726	34.9	1.1	−0.1	0.88	0.88	vs11d
J1048+7143*	1044+719	10 48 27.6199	+71 43 35.938	42.3	2.4	−1.2	1.44	1.44	vs04j
J1048−4114	1045−188	10 48 38.271	−41 14 00.08	16.0	1.0	−0.5	0.32	0.16	
J1051−3138	1048−313	10 51 04.7775	−31 38 14.307	24.6	1.0	0.4	0.96	0.56	vs09y
J1051+2119	1049+215	10 51 48.7890	+21 19 52.313	62.2	1.3	0.0	1.28	0.72	vs07j
J1058+0133	1055+018	10 58 29.6052	+01 33 58.824	52.8	4.1	0.5	2.80	1.36	vs02l
J1058+1951	1055+201	10 58 17.901	+19 51 50.87	63.1	1.7	0.0	0.48	0.40	vs06x
J1058−8003	1057−797	10 58 43.3100	−80 03 54.162	−18.3	2.1	1.1			vs05h
J1107−4449	1104−445	11 07 08.6943	−44 49 07.618	14.2	3.3	1.0			vs02v
J1118−4634	1116−462	11 18 26.9577	−46 34 15.001	13.4	1.9	0.2			vs05z
J1118+1234	1116+128	11 18 57.3014	+12 34 41.718	63.9	2.0	0.3	1.28	0.64	vs05s
J1125+2610	1123+264	11 25 53.7119	+26 10 19.979	70.9	1.1	0.0	1.04	0.96	vs09f
J1127−1857	1124−186	11 27 04.3924	−18 57 17.440	39.6	1.6	1.7	1.12	1.12	vs07i
J1130−1449*	1127−145	11 30 07.0525	−14 49 27.387	43.6	5.5	−0.6	3.60	0.64	vs01z
J1139−1350*	1136−135	11 39 10.703	−13 50 43.64	45.4	1.8	−0.7	0.24	< 0.10	
J1145−4836	1143−383	11 45 30.82	−48 36 12.1	12.8	1.4	−0.5	< 0.10	< 0.10	
J1146−2447	1143−245	11 46 08.1033	−24 47 32.896	35.7	1.5	0.2	1.36	0.72	vs06w
J1146−3328	1143−331	11 46 28.452	−33 28 42.66	27.5	1.1	0.1	0.24	< 0.10	
J1147−3812	1144−379	11 47 01.3706	−38 12 11.022	23.0	2.2	1.0	2.00	1.20	vs04d
J1147−0724	1145−071	11 47 51.5540	−07 24 41.140	52.2	1.2	−0.5	0.88	0.56	vs09x
J1150−0023	1148−001	11 50 43.8707	−00 23 54.204	58.8	2.0	−0.5	1.44	0.32	vs05r
J1153+4931	1150+497	11 53 24.4666	+49 31 08.830	65.0	1.0	0.0	0.96	0.72	vs09w
J1153+8058	1150+812	11 53 12.4993	+80 58 29.154	35.8	1.4	0.1	1.36	1.04	vs06v
J1158+2450	1155+251	11 58 25.7875	+24 50 17.963	77.9	1.2	0.0	0.80	0.16	

Table 1. (Continued.)

Source name J2000	Source name Common	R.A. J2000	Declination J2000	b (°)	S_5 (Jy)	α	S_{2M} (Jy)	S_{140M} (Jy)	Observation code
J1159+2914	1156+295	11 59 31.8339	+29 14 43.827	78.4	1.8	−0.1	1.76	1.76	vs05b
J1205−2634	1203−262	12 05 33.213	−26 34 04.45	35.2	1.1	−0.3	0.32	0.32	vs11c
J1209−2406	1206−238	12 09 02.446	−24 06 20.75	37.8	1.1	1.3	0.72	0.32	vs11b
J1215−1731	1213−172	12 15 46.7517	−17 31 45.403	44.5	1.8	0.5	1.76	1.76	vs05a
J1215+3448	1213+350	12 15 55.6010	+34 48 15.221	79.2	1.1	0.0	0.80	0.24	
J1218−4600	1215−457	12 18 06.2531	−46 00 29.014	16.5	2.4	−0.5			vs04h
J1219+4829	1216+487	12 19 06.4147	+48 29 56.165	67.7	1.0	0.0	0.88	0.56	vs11a
J1224+0330	1222+037	12 24 52.4218	+03 30 50.293	65.5	1.2	0.0	1.04	0.56	vs09e
J1224+2122	1222+216	12 24 54.458	+21 22 46.39	81.7	1.4	0.0	1.44	1.44	vs06o
J1225+1253	3C 272.1	12 25 03.743	+12 53 13.14	74.5	3.6	−0.3	0.24	0.16	
J1229+0203	3C 273B	12 29 06.6997	+02 03 08.598	64.4	43.6	0.0	32.00	0.80	vs01b
J1230+1223*	3C 274	12 30 49.4233	+12 23 28.044	74.5	61.2	−1.2	2.80	0.48	vs01a
J1232−0224	1229−021	12 32 00.016	−02 24 04.80	60.1	1.0	−0.3	0.64	0.24	
J1239−1023	1237−101	12 39 43.062	−10 23 28.70	52.4	1.3	−0.2	1.28	0.24	
J1242−0446*	3C 275	12 42 19.5294	−04 46 18.908	58.0	1.0	−1.0	< 0.10	< 0.10	
J1246−0730	1243−072	12 46 04.2320	−07 30 46.574	55.3	1.1	0.1	0.88	0.64	vs10z
J1246−2547	1244−255	12 46 46.8020	−25 47 49.288	37.1	2.3	0.9	1.12	0.48	vs04r
J1256−0547	3C 279	12 56 11.1665	−05 47 21.523	57.1	13.0	0.1	10.40	2.00	vs01g
J1257−3155	1255−316	12 57 59.0607	−31 55 16.851	30.9	1.4	−0.1	1.36	1.04	vs06u
J1305−1033	1302−102	13 05 33.0149	−10 33 19.427	52.2	1.0	−0.2	0.80	0.32	vs11q
J1309+1154	1307+121	13 09 33.9324	+11 54 24.552	74.2	1.3	0.0	0.72	0.32	vs09d
J1310+3220	1308+326	13 10 28.6638	+32 20 43.783	83.3	3.6	0.0	3.60	2.88	vs02e
J1316−3338	1313−333	13 16 07.9859	−33 38 59.172	28.9	1.6	0.2	1.60	0.96	vs05q
J1325−4301*	Cen A	13 25 27.6158	−43 01 08.803	19.4	200.0	−0.8	3.76	< 0.10	
J1331+3030*	3C 286	13 31 08.2881	+30 30 32.959	80.7	6.3	−0.8	3.36	< 0.10	
J1332+0200	1330+022	13 32 53.271	+02 00 45.70	63.0	1.5	−0.4	0.48	< 0.10	
J1337−1257	1334−127	13 37 39.7827	−12 57 24.692	48.4	4.4	0.6	4.40	4.00	vs01y
J1347+1217	1345+125	13 47 33.3616	+12 17 24.238	70.2	3.1	−0.3	1.28	0.24	
J1351−1449	1349−145	13 51 52.650	−14 49 14.56	45.6	1.1	0.0	0.56	0.40	vs10y
J1354−1041	1352−104	13 54 46.519	−10 41 02.66	49.2	1.0	−0.2	0.48	0.24	
J1357+1919	1354+195	13 57 04.4366	+19 19 07.372	73.0	2.7	0.9	1.04	0.40	vs03x
J1357−1744	1354−174	13 57 06.074	−17 44 01.91	42.4	1.1	−0.4	1.12	0.40	vs08j
J1405+0415	1402+044	14 05 01.1198	+04 15 35.819	61.2	1.0	0.1	0.88	0.88	vs10x
J1407+2827	OQ 208	14 07 00.3944	+28 27 14.690	73.3	2.4	0.5	2.40	0.80	vs03o
J1408−0752	1406−076	14 08 56.4811	−07 52 26.665	50.3	1.0	−0.1	0.72	0.64	vs11p
J1411+5212*	3C 295	14 11 20.6477	+52 12 09.141	60.8	7.4	−0.9	< 0.10	< 0.10	
J1415+1320	1413+135	14 15 58.8174	+13 20 23.713	65.9	1.2	0.3	0.88	0.88	vs09v
J1419+5423	1418+546	14 19 46.5974	+54 23 14.787	58.3	1.7	1.2	0.64	0.24	
J1419−1928	1417−192	14 19 49.739	−19 28 25.27	38.7	1.0	−0.1	0.40	0.32	vs11o
J1424−4913	1421−490	14 24 33.9	−49 13 59.0	10.9	5.8	−0.3			vs01v
J1427−4206	1424−418	14 27 56.2975	−42 06 19.437	17.3	3.8	0.0	3.36	2.96	vs02i
J1430+1043	1427+109	14 30 09.739	+10 43 26.86	61.6	1.2	0.0	1.04	0.96	vs09c
J1435−4821	1438−481	14 35 17.7	−48 21 52.0	11.0	1.1				vs10o
J1436+6336	1435+638	14 36 45.8021	+63 36 37.866	49.7	1.1	0.0	1.12	0.40	vs08i
J1445+0958	1442+101	14 45 16.4651	+09 58 36.072	58.2	1.2	0.0	0.96	0.16	
J1454−3747	1451−375	14 54 27.4097	−37 47 33.144	19.0	2.4	0.2	2.40	1.76	vs03n
J1501−3918	1458−391	15 01 34.757	−39 18 39.45	17.0	1.2		0.96	< 0.10	
J1504+1029	1502+106	15 04 24.9797	+10 29 39.198	54.6	1.8	−0.1	1.76	0.96	vs04z
J1506+3730	1504+377	15 06 09.5299	+37 30 51.132	59.9	1.0	0.0	0.88	0.80	vs10w
J1507−1652	1504−166	15 07 04.7869	−16 52 30.266	35.1	2.8	0.4	2.40	0.96	vs03m

Table 1. (Continued.)

Source name J2000	Source name Common	R.A. J2000	Declination J2000	b (°)	S_5 (Jy)	α	S_{2M} (Jy)	S_{140M} (Jy)	Observation code
J1510−0543*	1508−055	15 10 53.591	−05 43 07.42	42.9	1.7	−0.9	0.56	0.56	vs06t
J1512−0905	1510−089	15 12 50.5329	−09 05 59.829	40.1	3.3	0.1	2.24	1.20	vs02x
J1513−1012	1511−100	15 13 44.8934	−10 12 00.263	39.2	1.2	1.3	0.88	0.56	vs09u
J1516+0015	1514+004	15 16 40.219	+00 15 01.91	46.0	1.6	−0.2	0.88	0.80	vs07h
J1517−2422	1514−241	15 17 41.8131	−24 22 19.475	27.6	2.2	0.0	2.24	1.20	vs03u
J1522−2730	1519−273	15 22 37.6759	−27 30 10.785	24.4	2.3	−0.1	1.76	1.76	vs04q
J1526−1351	1524−136	15 26 59.440	−13 51 00.17	34.3	1.3	−0.4	0.80	< 0.10	
J1530−4231	1526−423	15 30 14.70	−42 31 57.0	11.3	1.4		< 0.10	< 0.10	
J1534+0131	1532+016	15 34 52.4536	+01 31 04.206	43.2	1.3	0.0	1.04	0.24	
J1540+1447	1538+149	15 40 49.4915	+14 47 45.884	48.8	1.2	0.0	0.88	0.80	vs09t
J1543−0757	1540−077	15 43 01.687	−07 57 06.65	35.6	1.0	−0.3	0.88	< 0.10	
J1546+0026	1543+005	15 46 09.5317	+00 26 24.645	40.3	1.3	0.0	0.96	0.32	vs09b
J1549+0237	1546+027	15 49 29.4368	+02 37 01.163	40.9	1.5	0.0	1.52	1.52	vs06e
J1550+0527	1548+056	15 50 35.2692	+05 27 10.448	42.2	3.3	1.0	2.80	2.40	vs02r
J1554−2704*	1550−269	15 54 02.468	−27 04 40.23	20.3	1.0	−0.6	0.48	< 0.10	
J1556−7914	1549−790	15 56 58.8705	−79 14 04.283	−19.5	4.7	−0.1			vs02d
J1557−0001	1555+001	15 57 51.4339	−00 01 50.413	37.7	2.3	−0.3	1.12	0.96	vs04p
J1602+3326	1600+335	16 02 07.2634	+33 26 53.072	48.7	2.0	−0.3	1.76	1.12	vs04y
J1608+1029	1606+106	16 08 46.2031	+10 29 07.775	40.8	1.7	0.7	1.28	0.64	vs06s
J1613+3412	1611+343	16 13 41.0642	+34 12 47.908	46.4	4.0	0.0	4.00	2.00	vs02b
J1615−6039*	1610−607	16 15 15.8	−60 39 14.0	−7.0	8.4	−1.2	0.08	0.08	
J1617−7717	1610−771	16 17 49.2768	−77 17 18.467	−18.9	3.3	0.0			vs02u
J1624−6809	1619−680	16 24 18.4373	−68 09 12.498	−13.0	2.1	0.3			vs05g
J1625−2527	1622−253	16 25 46.8916	−25 27 38.326	16.3	3.5	0.7	3.36	3.04	vs02h
J1625+4134	1624+416	16 25 57.6697	+41 34 40.629	44.2	1.4	0.0	1.04	0.16	
J1626−2951	1622−297	16 26 06.0208	−29 51 26.971	13.3	2.4	−0.2	2.40	1.20	vs03l
J1635+3808	1633+382	16 35 15.4929	+38 08 04.500	42.3	3.2	0.4	2.16	0.40	vs03d
J1637+4717	1636+473	16 37 45.1307	+47 17 33.836	41.9	1.3	0.0	0.80	0.40	vs09a
J1638+5720	1637+574	16 38 13.4563	+57 20 23.978	40.4	1.8	0.7	1.28	1.20	vs06n
J1640+3946	NRAO 512	16 40 29.6327	+39 46 46.028	41.4	1.3	0.3	0.80	0.56	vs08y
J1640+1220	1638+124	16 40 47.939	+12 20 02.08	34.5	1.3	0.0	0.72	0.32	vs08z
J1642+3948	3C 345	16 42 58.8099	+39 48 36.993	40.9	8.4	0.0	6.08	1.60	vs01k
J1642+6856	1642+690	16 42 07.8485	+68 56 39.756	36.6	1.5	−0.2	1.04	0.56	vs07w
J1642−0621	1639−062	16 42 02.177	−06 21 23.70	25.0	1.6		1.60	< 0.10	
J1644−7715	1637−771	16 44 17.6	−77 15 42.0	−20.0	2.5	−0.5	0.08	0.08	
J1647−6437	1642−645	16 47 37.2	−64 37 57.0	−12.5	1.3				vs08t
J1651+0459*	3C 348	16 51 08.16	+04 59 33.8	28.9	9.5	−1.5	< 0.10	< 0.10	
J1653+3945	Mrk 501	16 53 52.2166	+39 45 36.609	38.9	1.4	0.0	0.80	0.40	vs08h
J1658+4737	1656+477	16 58 02.7795	+47 37 49.231	38.4	1.4	0.0	0.80	0.72	vs08g
J1658+0741	1655+077	16 58 09.0114	+07 41 27.540	28.6	1.6	0.5	1.04	0.64	vs07g
J1658+0515	1656+053	16 58 33.4473	+05 15 16.444	27.4	2.1	0.0	1.04	0.56	vs05i
J1658−0739	1656−075	16 58 44.061	−07 39 17.70	20.8	1.3		1.28	< 0.10	
J1702−7741	1655−776	17 02 41.034	−77 41 57.0	−21.0	1.1	−0.4	0.16	0.16	
J1710+0036	1708+006	17 10 35.00	+00 36 45.0	22.6	1.1	0.0	< 0.10	< 0.10	
J1720−0058*	3C 353	17 20 28.164	−00 58 46.60	19.6	8.9	−1.1	< 0.10	< 0.10	
J1723−6500	1718−649	17 23 41.0295	−65 00 36.610	−15.8	4.4	0.2	1.60	0.80	vs02f
J1724−0241*	1722−026	17 24 36.65	−02 41 02.6	17.9	1.0	−0.8	< 0.10	< 0.10	
J1726−6427	1722−644	17 26 56.8	−64 27 51.0	−15.9	1.3				vs08s
J1727+4530	1726+455	17 27 27.6508	+45 30 39.731	33.3	1.3	0.0	1.28	0.96	vs07f
J1728+0427	1725+044	17 28 24.9527	+04 27 04.913	20.5	1.2	0.0	0.64	0.24	

Table 1. (Continued.)

Source name J2000	Common	R.A. J2000	Declination J2000	b (°)	S_5 (Jy)	α	S_{2M} (Jy)	S_{140M} (Jy)	Observation code
J1733−1304	NRAO 530	17 33 02.7057	−13 04 49.547	10.8	7.0	0.8	6.40	4.80	vs01m
J1734+3857	1732+389	17 34 20.5785	+38 57 51.442	31.0	1.3	0.0	1.28	0.96	vs07e
J1740+5211	1739+522	17 40 36.9778	+52 11 43.407	31.7	1.1	0.0	0.88	0.80	vs10v
J1743−0350	1741−038	17 43 58.8561	−03 50 04.616	13.1	2.4	0.3	2.40	1.60	vs03k
J1744−5144	1740−517	17 44 25.4506	−51 44 43.792	−11.5	3.9	−0.3			vs02p
J1745−0753	1742−078	17 45 27.104	−07 53 03.60	10.8	1.4		1.12	< 0.10	
J1751+0939	1749+096	17 51 32.8185	+09 39 00.728	17.6	2.3	1.4	0.80	0.80	vs04o
J1753+4409	1751+441	17 53 22.6479	+44 09 45.685	28.5	1.0	0.0	0.56	0.32	vs11n
J1800+7828	1803+784	18 00 45.6839	+78 28 04.018	29.1	2.6	0.4	2.64	1.92	vs02w
J1801+4404	1800+440	18 01 32.3149	+44 04 21.900	27.1	1.1	0.0	0.56	0.56	vs10u
J1804+0101	1801+010	18 04 15.984	+01 01 32.40	11.0	1.6	0.7	0.80	< 0.10	
J1806+6949	3C 371	18 06 50.6806	+69 49 28.108	29.2	2.2	0.2	1.20	0.32	vs04x
J1809−4552	1806−458	18 09 57.8719	−45 52 41.014	−12.5	1.1	−0.1			vs10n
J1819−5521	1815−553	18 19 45.4007	−55 21 20.741	−17.8	1.1	−0.3			vs10m
J1824+1044	1821+107	18 24 02.8552	+10 44 23.773	10.9	1.1	0.0	0.80	0.40	vs10t
J1824+5651	1823+568	18 24 07.0683	+56 51 01.490	26.1	1.5	0.0	1.52	1.52	vs06d
J1832+2833	1830+285	18 32 50.1856	+28 33 35.955	16.3	1.1	0.0	0.56	0.40	vs10s
J1833−2103*	1830−211	18 33 39.886	−21 03 40.57	−5.7	7.9	−0.3	2.88	< 0.10	
J1837−7108	1831−711	18 37 28.7146	−71 08 43.555	−24.5	2.3	0.9			vs04m
J1842+7946*	3C 390.3	18 42 08.9899	+79 46 17.127	27.1	1.0	−0.8	0.80	0.32	vs11m
J1902+3159	3C 395	19 02 55.9389	+31 59 41.701	11.8	1.9	−0.3	1.28	0.32	vs06c
J1911−2006	1908−201	19 11 09.6528	−20 06 55.108	−13.2	2.3	0.1	1.76	0.80	vs04n
J1912−8010	1903−802	19 12 40.0193	−80 10 05.947	−27.6	1.3	−0.3			vs08r
J1924−2914	1921−293	19 24 51.0559	−29 14 30.120	−19.6	14.8	0.7	14.80	7.60	vs01e
J1925+2106*	1923+210	19 25 59.6053	+21 06 26.161	2.3	1.5	+0.2	1.20	0.40	vs07v
J1927+7358	1928+738	19 27 48.4951	+73 58 01.569	23.5	3.6	0.1	3.20	1.20	vs02m
J1932−4546	1929−457	19 32 44.902	−45 46 37.75	−26.0	1.0	0.5			vs11k
J1937−3958	1933−400	19 37 16.2174	−39 58 01.553	−25.4	1.1	−0.3	1.12	0.64	vs08f
J1939−6342*	1934−638	19 39 25.0262	−63 42 45.625	−29.4	5.9	−1.1			vs01u
J1939−1525*	1936−155	19 39 26.6577	−15 25 43.057	−17.4	1.4	−1.0	1.44	1.44	vs06m
J1940−6907	1935−692	19 40 25.5282	−69 07 56.972	−29.6	1.0	−0.3			vs11j
J1949−1957	1946−200	19 49 53.420	−19 57 13.32	−21.5	1.3	0.6	1.12	< 0.10	
J1955+5131	1954+513	19 55 42.7382	+51 31 48.545	11.8	1.6	0.2	1.60	0.24	
J1957−3845	1954−388	19 57 59.8192	−38 45 06.356	−29.0	4.4	0.0	4.40	4.00	vs01x
J1959+4044*	Cyg A	19 59 28.357	+40 44 02.09	5.8	700.0	−0.7	0.80	0.16	
J2000−1748	1958−179	20 00 57.0904	−17 48 57.672	−23.1	1.8	0.2	1.76	1.76	vs04w
J2003−3251	2000−330	20 03 24.1162	−32 51 45.131	−28.6	1.2	1.0	1.04	0.40	vs08x
J2005+7752	2007+777	20 05 30.9984	+77 52 43.247	22.7	1.7	0.3	1.12	0.64	vs06r
J2009−4849	2005−489	20 09 25.3909	−48 49 53.719	−32.6	1.2	0.2			vs09n
J2011−1546	2008−159	20 11 15.7109	−15 46 40.253	−24.6	1.4	0.4	1.28	1.28	vs07d
J2022+6136	2021+614	20 22 06.6816	+61 36 58.804	13.8	3.0	0.4	3.04	0.96	vs02q
J2031+1219	2029+121	20 31 54.9942	+12 19 41.340	−15.8	1.2	0.0	1.04	0.72	vs08w
J2040−2507*	2037−253	20 40 08.7729	−25 07 46.662	−34.2	1.2	−0.6	0.48	0.40	vs09s
J2101+0341	2059+034	21 01 38.8341	+03 41 31.320	−26.6	1.3	0.0	0.96	0.32	vs08v
J2109−4110	2106−413	21 09 33.1885	−41 10 20.605	−42.8	2.3	0.0	2.16	1.20	vs03w
J2110−1020	2107−105	21 10 00.979	−10 20 57.32	−35.4	1.2	1.2	0.96	0.40	vs09r
J2115+2933	2113+293	21 15 29.4134	+29 33 38.366	−13.3	1.2	0.0	0.80	0.48	vs09q
J2123+0535	2121+053	21 23 44.5173	+05 35 22.093	−30.1	3.2	0.8	0.64	0.40	vs03c
J2129−1538	2126−158	21 29 12.1758	−15 38 41.040	−41.9	1.2	0.0	1.12	0.32	vs08e
J2131−1207	2128−123	21 31 35.2617	−12 07 04.795	−41.0	3.0	0.8	2.24	0.24	

Table 1. (Continued.)

Source name J2000	Common	R.A. J2000	Declination J2000	b (°)	S_5 (Jy)	α	S_{2M} (Jy)	S_{140M} (Jy)	Observation code
J2134−0153*	2131−021	21 34 10.3095	−01 53 17.238	−36.5	2.0	−1.0	1.44	0.32	vs05p
J2136+0041	2134+004	21 36 38.5863	+00 41 54.214	−35.6	12.4	0.5	8.80	0.80	vs01h
J2139+1423	2136+141	21 39 01.3092	+14 23 35.992	−27.5	2.0	0.0	2.00	0.48	vs04c
J2147+0929	2144+092	21 47 10.1629	+09 29 46.672	−32.3	1.1	0.0	0.88	0.32	vs10r
J2148+0657	2145+067	21 48 05.4586	+06 57 38.604	−34.1	6.4	0.4	6.40	2.40	vs01l
J2151+0552	2149+056	21 51 37.8754	+05 52 12.954	−35.4	1.0	0.0	0.88	0.32	vs10q
J2151−3027	2149−306	21 51 55.5239	−30 27 53.697	−50.8	1.4	0.0	1.44	0.24	
J2152−7807	2146−783	21 52 03.1546	−78 07 06.638	−35.2	1.1	0.5			vs10l
J2158−1501	2155−152	21 58 06.2818	−15 01 09.327	−48.0	3.1	1.1	2.40	0.40	vs03g
J2202+4216	BL Lac	22 02 43.2913	+42 16 39.979	−10.4	5.6	−0.2	5.60	0.80	vs01q
J2203+3145	2201+315	22 03 14.9757	+31 45 38.269	−18.8	2.9	0.6	2.08	0.24	
J2206−1835	2203−188	22 06 10.4150	−18 35 38.762	−51.2	4.3	−0.4	0.96	< 0.10	
J2207−5346	2204−540	22 07 43.7333	−53 46 33.817	−49.9	1.4	−0.5			vs08d
J2209−2331*	2206−237	22 09 20.10	−23 31 52.4	−53.3	1.0	−0.6	< 0.10	< 0.10	
J2212+2355	2209+236	22 12 05.9662	+23 55 40.543	−26.1	1.4	0.0	1.44	0.32	vs06l
J2213−2529	2210−257	22 13 02.4970	−25 29 30.082	−54.6	1.0	−0.3	0.72	0.16	
J2218−0335	2216−038	22 18 52.0377	−03 35 36.879	−46.6	2.7	0.4	2.40	0.48	vs03j
J2225+2118	2223+210	22 25 38.048	+21 18 06.40	−30.1	1.2	0.0	0.64	< 0.10	
J2225−0457	3C 446	22 25 47.2592	−04 57 01.390	−48.8	6.4	0.5	2.40	0.48	vs01s
J2229−0832	2227−088	22 29 40.0843	−08 32 54.434	−51.7	2.4	0.8	1.44	0.80	vs04i
J2230+6946	2229+695	22 30 36.4697	+69 46 28.076	10.2	1.4	0.0	0.40	< 0.10	
J2230−3942*	2227−399	22 30 40.2786	−39 42 52.067	−58.3	1.0	−1.0	0.40	< 0.10	
J2232+1143*	CTA 102	22 32 36.4088	+11 43 50.904	−38.6	4.4	−0.6	4.40	0.32	vs01w
J2235−4835	2232−488	22 35 13.2370	−48 35 58.792	−56.1	1.1	0.5			vs10k
J2236+2828	2234+282	22 36 22.4708	+28 28 57.413	−25.7	1.6	0.7	1.12	0.32	vs07c
J2239−5701	2236−572	22 39 11.9	−57 01 01.0	−52.0	1.1	1.5	< 0.10	0.40	vs10p
J2243−2544	2240−260	22 43 26.408	−25 44 30.68	−61.4	1.2	0.2	0.24	< 0.10	
J2246−1206	2243−123	22 46 18.2319	−12 06 51.277	−57.1	2.7	0.0	2.08	0.72	vs03v
J2249+1136	NGC 7385	22 49 54.586	+11 36 30.84	−41.3	1.1	0.0	< 0.10	< 0.10	
J2250+1419	2247+140	22 50 25.5400	+14 19 50.600	−39.2	1.2	0.0	< 0.10	< 0.10	

The PIs were unanimous in giving permission for such GOT/Survey extractions.

4. The VSOP Survey Ground Resources

The HALCA on-board hardware, telemetry and tracking station systems, and the data correlation are described elsewhere (Hirabayashi et al. 1998; Hirabayashi et al. 2000). Both the GOT and the VSOP Survey observations require a large effort and the cooperation of numerous ground resources, which are described below.

4.1. The Ground Telescopes

A typical GOT observation uses HALCA with six to nineteen ground telescopes, observing for a duration of about 10 hr, or about two orbits of the spacecraft. These data generally produce images of high quality. The ground telescope time for these observations was arranged before the mission by the Global VLBI Working Group (GVWG). The VSOP Survey, on the other hand, was designed to observe using $\sim$ 3 telescopes with an observation length of about one orbit. These more minimal resources made it possible for the survey to negotiate for sufficient additional ground resources *after* telescope allocations were made for the GOT experiments.

The telescopes (with supporting institution, country, and total survey observing time in days in 1998–1999) are as follows: Arecibo (NAIC, Puerto Rico, 1.7 d); Ceduna and Hobart (University of Tasmania, Australia, 1.2 d, 10.8 d); Green Bank 140-ft (NRAO, USA, 3.7 d); Hartebeesthoek (Hartebeesthoek Radio Astronomy Observatory, South Africa, 12.5 d); Kalyazin (Lebedev Physical Institute, Russia, 1.4 d); Kashima (CRL, Japan, 4.0 d); Mopra (ATNF, Australia, 10.5 d); Noto (CNR, Italy,

Table 1. (Continued.)

Source name J2000	Common	R.A. J2000	Declination J2000	b (°)	S_5 (Jy)	α	S_{2M} (Jy)	S_{140M} (Jy)	Observation code
J2253+1608	3C 454.3	22 53 57.7479	+16 08 53.563	−38.2	16.0	0.6	16.00	4.80	vs01d
J2255+4202	2253+417	22 55 36.7078	+42 02 52.532	−15.8	1.1	0.0	0.88	0.24	
J2257−3627	2254−364	22 57 10.9	−36 27 55.0	−64.1	1.1	0.6			
J2258−2758	2255−282	22 58 05.9628	−27 58 21.256	−64.9	2.5	0.7	2.48	1.76	vs03f
J2311+3425	2308+341	23 11 05.329	+34 25 10.90	−24.0	1.0	0.0	0.72	0.24	
J2320+0513	2318+049	23 20 44.8566	+05 13 49.952	−50.9	1.2	0.0	0.88	0.64	vs09p
J2321+2732	2319+272	23 21 59.8622	+27 32 46.443	−31.3	1.0	0.0	0.80	0.24	
J2329−4730	2326−477	23 29 17.7043	−47 30 19.115	−64.1	2.2	−0.2			vs04t
J2330+1100	2328+107	23 30 40.8522	+11 00 18.710	−47.1	1.2	0.0	1.20	0.24	
J2331−1556	2329−162	23 31 38.6524	−15 56 57.008	−68.4	1.9	1.1	1.20	0.48	vs06b
J2333−2343	2331−240	23 33 55.2378	−23 43 40.657	−72.2	1.1	−0.2	0.72	0.16	
J2336−5236	2333−528	23 36 12.1448	−52 36 21.950	−60.9	1.6	0.3			vs07b
J2339−3310*	2337−334	23 39 54.533	−33 10 16.90	−73.4	1.2	−1.5	0.56	< 0.10	
J2341−5816	2338−585	23 41 17.7	−58 16 10.0	−56.5	1.1	−0.4			vs10j
J2346+0930	2344+092	23 46 36.8385	+09 30 45.515	−50.1	1.4	0.0	1.28	0.24	
J2348−1631*	2345−167	23 48 02.6085	−16 31 12.021	−71.9	2.6	−0.9	2.56	1.28	vs03b
J2354+4553	2351+456	23 54 21.6802	+45 53 04.236	−15.8	1.2	0.0	1.20	0.24	
J2355+4950*	2352+495	23 55 09.4581	+49 50 08.340	−12.0	1.5	−0.6	1.20	0.16	
J2357−1125	2354−116	23 57 31.197	−11 25 39.18	−69.8	1.4	−0.2	1.36	0.24	
J2357−5311	2355−534	23 57 53.2661	−53 11 13.690	−62.1	1.8	0.5			vs06j
J2358−1020	2355−106	23 58 10.8824	−10 20 08.610	−69.0	1.6	2.1	1.44	1.44	vs06k
J2358−6054*	2356−611	23 58 56.3	−60 54 22.0	−55.1	6.0	−1.2	0.08	0.08	

5.0 d); Sheshan (Shanghai Astronomical Observatory, China, 9.7 d); Torun (Nicolaus Copernicus University, Poland, 3.7 d); Usuda (ISAS, Japan, 3.8 d). Telescopes participating only in GOT observations, indirectly contributing to the survey observations via data extractions, are: ATCA (ATNF, Australia, 1.5 d); Effelsberg (MPIfR, Germany, 2.7 d); Jodrell Bank MKII (MERLIN/VLBI National Facility, UK, 0.5 d); VLBA (NRAO, USA, 7.0 d using three of ten telescopes).

4.2. The Tracking Stations and Correlators

The ISAS Space Center facility near Kagoshima, Japan is the command and control center of HALCA. For telemetry between the ground and HALCA, five tracking stations are used: one tracking station is operated by ISAS at Usuda, Japan; three stations by the NASA Deep Space Network (DSN) at Goldstone, CA, USA, Robledo, Spain, and Tidbinbilla, Australia; and one station in Green Bank, WV, USA, operated by NRAO and supported by NASA.

HALCA data, recorded at a tracking station, are shipped to one of the three correlation centers where they are correlated with ground-telescope data, approximately one month after the observations. An updated HALCA orbit, determined by JPL and by ISAS, is also supplied. The three correlators are: the VSOP correlator in Mitaka, Japan (Shibata et al. 1998); the S2 correlator in Penticton, BC, Canada (Carlson et al. 1999); and the VLBA correlator in Socorro, NM, USA (Napier et al. 1994). More detailed information concerning the tracking stations and correlators are given by Hirabayashi et al. (2000).

Because the VSOP Survey Programme was designed to use telescopes with S2- or VSOP-recording systems, most survey observations were correlated in Penticton or in Mitaka. However, the VLBA correlator is also used for data extracted from GOT experiments correlated in Socorro.

5. The VSOP Survey Experiments

5.1. The Observations and Correlations

Sources in the VSS are observed in the following way. The GOT observations are first scheduled and then survey observations are placed to make HALCA relatively efficient. The priority ordering in scheduling of the survey observations is from the strongest sources to the weakest sources. However, constraints of when a source can be observed with HALCA somewhat randomizes the selection process. About one in three HALCA observations

(including GOT extractions) is a survey observation, and these account for about 25% of the total on-source observing time. A typical survey observation consists of five hours of data, about one HALCA orbit, scheduled with three well-separated ground telescopes. About 100 of the 289 sources are also in GOT proposals, and a typical amount of survey data (three ground telescopes over five hours) are extracted at the correlator from these observations.

The ground array that is scheduled with HALCA for survey observations depends on the source declination. Sources south of $-30°$ use telescopes in Australia (Mopra, Hobart, Ceduna) and Hartebeesthoek in South Africa. For more Northern declinations telescopes in Eastern Asia (Shanghai, Usuda, Kashima) or telescopes in the Europe–Atlantic region (Hartebeesthoek, Noto, Torun, Kalyazin, Green Bank 140-ft, Arecibo) are also included. Generally, four ground telescopes are scheduled for each experiment, although usually only three (and sometimes two) telescopes are available for the observations.

A majority of the VSOP Survey observations were correlated with the Penticton correlator, since the majority of telescopes record the data in the S2 format. Those observations which included Usuda and/or Kashima were often correlated with the Mitaka correlator. Approximately 30% of the survey observations are GOT observations from which a representative amount of Survey data were extracted. Many of these GOT experiments were scheduled with the VLBA and the EVN (European VLBI Network), and the extractions and correlations were made with the VLBA correlator.

5.2. *The Data Calibration and Editing*

A complete discussion of the procedures for reducing the VSOP Survey observations has been given by Moellenbrock et al. (2000). The data are taken in two 16-MHz bandwidths in left-circular-polarization at sky frequencies between 4.80 and 5.00 GHz. Each of the two bandwidths is split into at least 128 frequency channels and the data sampled every 0.5 s with HALCA baselines and every 2.0 s with the ground baselines. Data from any of the three correlators are then written in FITS format and then sent to ISAS for distribution to the various Survey Reduction Team members.

The following reduction and editing steps are generally performed in AIPS, the NRAO reduction package used for interferometric data. The first calibration step is an a priori gain calibration of HALCA and the ground telescopes using the measured system temperatures as well as the telescope gain curves; the antenna sensitivities are generally accurate to about 20% of their nominal values. Gross editing of the data, based on reports from the telescopes and correlators, is also made.

Fringe-fitting of the HALCA baselines is one of the most important parts of the survey reductions. Without the detection of HALCA fringes, the data are useless for further reductions, except to estimate an upper limit of the correlated flux densities from the space baselines. Detections are difficult because of: 1) the relatively low correlated flux densities on space baselines, often not much above detection limit of about 0.1 Jy; 2) the limited sensitivity of HALCA; 3) the uncertainties in the orbit; 4) the uncertainties in the timing parameters associated with the tracking stations; 5) the variable coherence time; 6) the large data base which is needed for fringe searching in large delay and rate windows.

Generally, the two 16 MHz bandwidths are fringe-fit independently. A satisfactory fringe-fit is obtained if the delay and rate solutions are relatively continuous in time, the estimated signal-to-noise ratio is large (the value depends on many of the fringe-fitted parameters and is typically > 4 for a secure detection) and the difference in solutions between the two bandwidths is small.

If fringes are not detected with HALCA baselines, then a comparison of the upper-limit visibility amplitude from the space baselines with the visibility amplitude from the ground baselines (almost always detected) can determine if the source is really resolved or if there may have been a problem with the HALCA data. If the source is detected with space baselines, a comparison of the visibility amplitude from the HALCA baselines with that from the ground baselines, or with pre-existing VLBI ground images, can be used to improve the amplitude calibration of all telescopes. Additional editing of the data during any unexpected loss of signal is also made at this stage of fringe-fitting.

5.3. *Further Processing and Results*

After successful fringe-fitting in AIPS, the data are averaged to 30 s time samples for each bandwidth and further reductions are made using the Difmap software system (Shepherd 1997). The basic products from a VSOP Survey observation are: (1) the correlated visibility amplitude as a function of the projected (u, v) spacing and (2) an image and model of the radio source with a resolution of about 0.2 mas $\times$ 0.4 mas. One of the more important parameters associated with the radio structure is the component brightness temperature or lower limit, which is proportional to the flux density in the component divided by its angular size. With a sufficient signal-to-noise ratio and with relatively simple source structures, the angular sizes or limits can be determined to about 10% of the resolution. For most sources, however, the typical diameter limits are about 20% of the resolution. Some examples are given in section 6.

5.4. *VSOP Survey Status and Supporting Observations*

As of 2000 July, 198 of the 289 VSS sources (69%) had been observed. For about 40 of the observations, only two ground telescopes were available; nonetheless, most of these have produced useful images and models. About 10% of the observations appear faulty (no signal was detected from HALCA although there were strong fringes from ground baselines) and these will be rescheduled if possible.

The results from the VSOP Survey Programme will be enhanced by a comparison with other ground observational results, across the entire electromagnetic spectrum. Additional information is: (1) radio source variability (e.g., Kovalev et al. 2000; Tingay et al. in preparation); (2) the arcsec radio structure of the sources; (3) VLBA 15 GHz observations within two months of the VSOP Survey observations (Gurvits et al. in preparation); and (4) a compilation of relevant radio/optical/X-ray data associated with each source in a convenient database.

6. Selected VSOP Survey Results

6.1. *VSOP Survey Data Base*

The results from the VSOP Survey will provide a source list which will be used for future space VLBI missions, such as RadioAstron (Kardeshev 1997), ARISE (Ulvestad, Linfield 1998) and VSOP-2 (Hirabayashi 2000). The efficient design of the resolution and sensitivity of these future SVLBI missions will rely on the statistical properties of the sources which are being studied in the VSOP Survey Project. In addition, the Survey results, when incorporated with much other astronomical information, will add to the understanding of many astrophysical phenomena. For these reasons, the mission has undertaken to document and catalog the VSOP Survey results as clearly, comprehensively and conveniently as possible.

The mammoth effort to reduce and image the VSOP Survey observations has been undertaken by a global community of astronomers, with the following main contributors: S. Horiuchi (NAO), Z. Shen (NAO), W. Scott (Calgary), S. Dougherty (Penticton), J. Lovell (ATNF), R. Dodson (Tasmania), S. Tingay (ATNF), L. Gurvits (JIVE), M. Lister (JPL), G. Piner (JPL), G. Moellenbrock (NRAO), E. Fomalont (NRAO). A comprehensive documentation of the crucial calibration steps and the final images, modelfits and other parameters are available from a database designed by J. Lovell, which can be accessed from http://www.vsop.isas.ac.jp/survey. Information associated with the data reduction and calibration, and useful templates are also available from this website.

As an example of the typical output from the survey observations, the results associated with two observations (vs03s for J0106−40 and vs10d for 0745+241) are shown in figure 1 (reproduced from Moellenbrock et al. 2000). The source 0745+241 consists of two major components. The brighter component contains 0.33 Jy with an angular size of 0.36 mas × < 0.06 mas at a position angle of 119°, corresponding to a brightness temperature limit of $> 0.8 \times 10^{12}$ K. Because the (u, v) tracks for many of the survey observations are significantly elliptical, a component is often resolved in the direction of best resolution, but unresolved in the orthogonal direction. The fainter component has a flux density of 0.03 Jy and is located 3.4 mas in position angle −60° from the brighter component. This faint component is resolved with an approximate angular size of 0.3 mas and a brightness temperature of 0.05×10^{12} K.

The best model-fit to J0106−40 is a single Gaussian component with a flux density of 3.1 Jy in an angular size of 0.29 mas × 0.18 mas at a position angle of 180°, corresponding to a brightness temperature of 2.8×10^{12} K. The maximum brightness temperature limit that can be measured from these observations is about 6×10^{12} K, corresponding to a few Jy within a 0.10 mas component. Because many of the sources contained unresolved or barely resolved components, simulations were made to determine realistic limits in the presence of the calibration errors and relatively poor (u, v) coverage with the survey observations (Lovell et al. 2000).

6.2. *The Statistical Properties of AGN Angular Sizes*

One of the most anticipated and basic results from the VSOP Survey is the distribution of the normalized visibility amplitude of AGN at the sub-mas level. This statistic is directly related to the average angular size distribution and, hence, the brightness temperature distribution, and will be used as a test of models of superluminal ejection in AGN which produce the apparent high brightness temperatures well in excess of 10^{12} K. With space baselines about a factor of three longer than available from ground-based VLBI, the brightness temperature sensitivity with HALCA is at least a factor of five better. The distribution also indicates whether future space missions with even more resolution than that of VSOP will be able to detect an appreciable number of sources for further studies.

The distribution of the normalized visibility amplitude form the first 67 sources fully reduced from the VSOP Survey are shown in figure 2 (reproduced from Lovell et al. 2000). The distribution has been normalized to unity for the average visibility amplitude at 30 Mλ. Based on the statistical results from the VLBApls survey (Fomalont et al. 2000b), the average visibility at 30 Mλ divided by the total flux density is 0.57. At 200–250 Mλ, the visibility amplitude drops more slowly, indi-

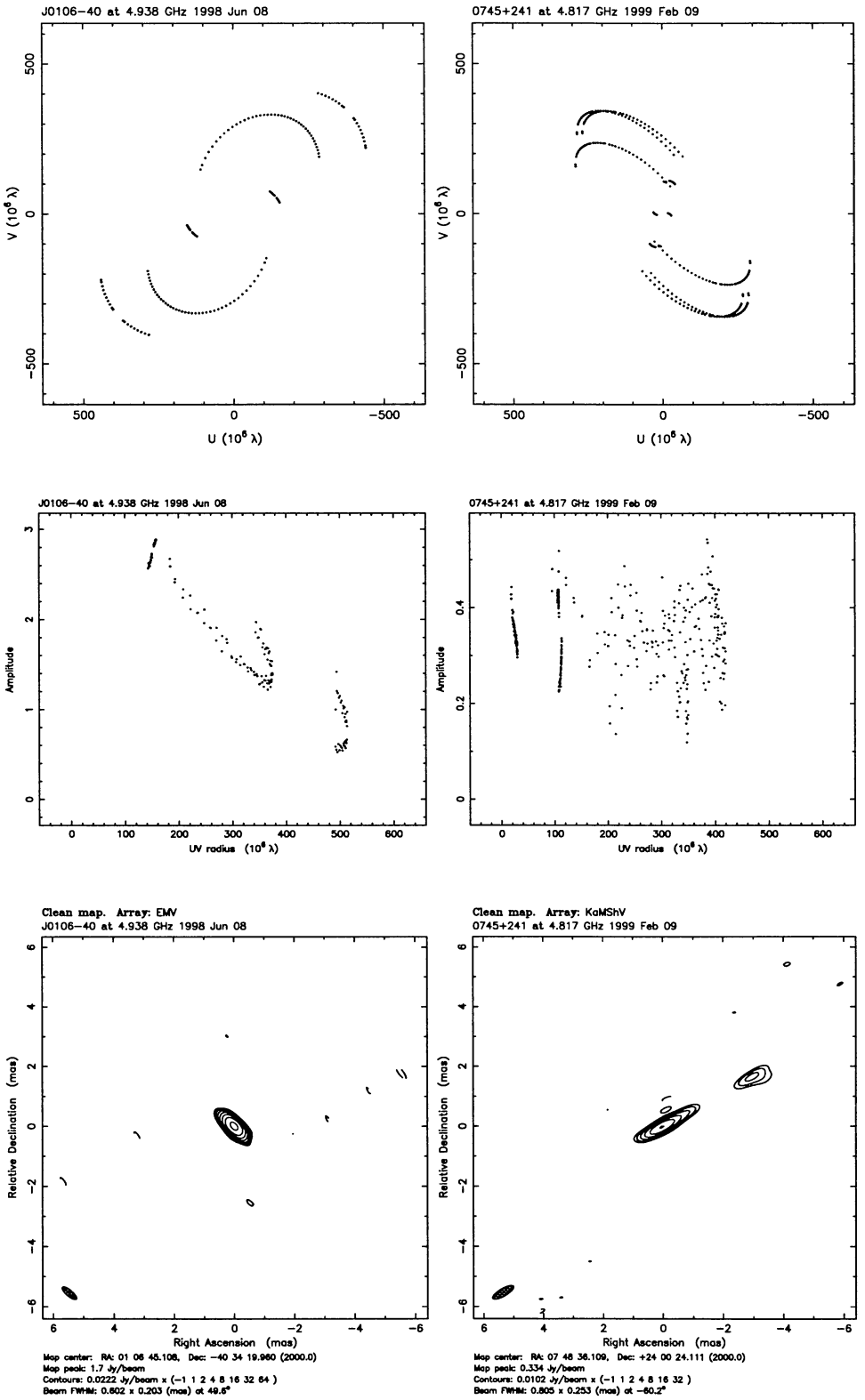

Fig. 1. Typical results for two survey sources: (Top) the (u, v) coverages; (Middle) the visibility plots; (Bottom) the images. The left panel is for survey source J0106−40 at epoch 1998.43. The ground telescopes were Hobart and Hartebeesthoek, the tracking station was Madrid, the correlator was Penticton, and the on-source time was 6.3 hr. The right panel is for survey source 0745+241 at epoch 1999.11. The ground telescopes used were Kashima, Mopra and Shanghai, the tracking station was Usuda, the correlator was Mitaka, and the total on-source time was 5.3 hr.

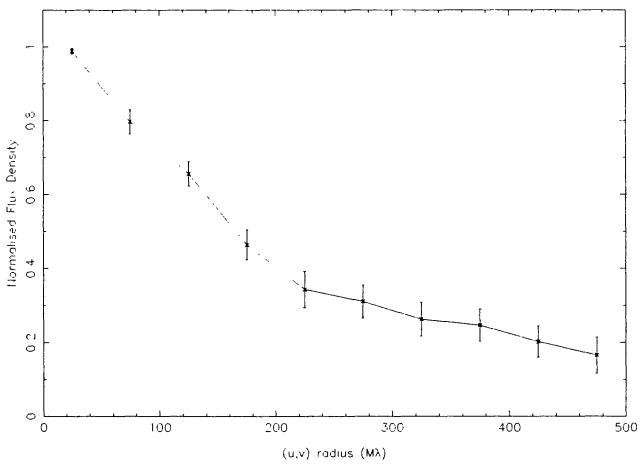

Fig. 2. Weighted mean of the normalized correlated flux density distribution for 67 survey sources. The error bars indicate the rms error of each point. The distribution has been normalized to 1.0 at 30 Mλ.

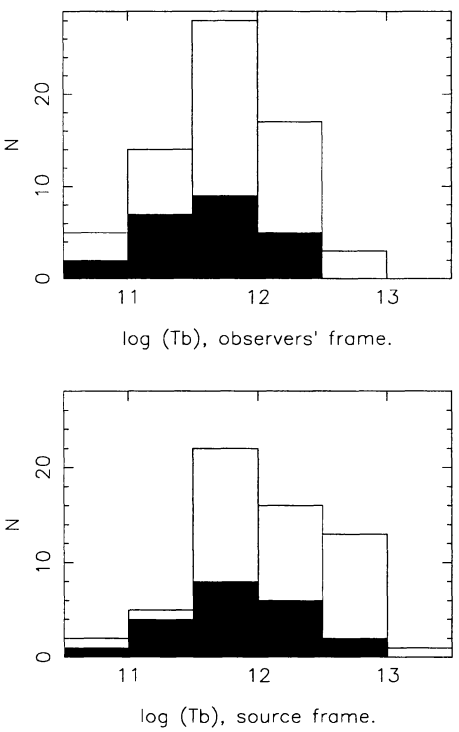

Fig. 3. Brightness temperature distribution for survey sources: (Top) in the observers' frame for the sample of 67 sources; (Bottom) in the source frame for the 59 sources with redshifts. The filled blocks represent sources where a compact component size was measured, while the open blocks represent sources where only a size upper limit, and hence brightness temperature lower limit, is available.

cating that a less-resolved component tends to dominate on the space-VLBI scale at 5 GHz and that most of the more extended structure is resolved out. A similar measure of the smallness of the typical AGN radio core is that 15% of the sample show no appreciable decrease in correlated flux density between 200 Mλ and 500 Mλ.

Figure 3 shows the brightness temperature distributions from the 67 sources analyzed so far. The highest observer-frame brightness temperature so far measured in the survey is 2.8×10^{12} K, and the highest lower-limit is 6×10^{12} K. We find that 30% of the 67 sources have observer-frame brightness temperatures in excess of 10^{12} K and for the 59 sources for which redshifts are available, 51% have source-frame brightness temperatures greater than 10^{12} K.

The above results clearly show that it is more than the occasional peculiar radio source which has a component with a brightness temperature equal to or larger than the standard 'inverse-Compton limit' and much larger than the limit based on equi-partition of energy considerations in radio sources. (Based on these results, we estimate that about 15% of the VSOP all-sky survey flat-spectrum sample may have such a component.) Although the superluminal motion in many of these sources strongly suggests that the high brightness temperatures are associated with Doppler beaming of the components nearly in the line of sight, there is at present no good statistical body of data which can test various competing theories which incorporate the radiative limits of high brightness regions, the distribution and lifetime of superluminal motions, and the connection with short-term variability in many of these sources. It is only with space VLBI that brightness temperatures significantly in excess of 10^{12} K can be measured and compared successfully with the high brightness temperature phenomena in active galaxies and inner jet regions.

6.3. *Supporting Ground Observations*

The results from the VSOP Survey will be enhanced by comparisons with observational results at other wavelengths. Some of these observations have been proposed specifically to support the VSOP Survey. As an example, figure 4 shows the comparison of a VSOP 5 GHz Survey image with a VLBA 15 GHz image for the source J2246−12 (=2243−123) (Kellermann et al. 2000), at the same resolution. Similar features are seen at the two frequencies: The brighter component has a flux density of 1.66 Jy at 15 GHz and 0.48 Jy at 4.9 GHz and is more extended in the North–South direction; The component to the north has an angular size of about 0.6 mas with a flux density of 0.16 Jy at 15 GHz and 0.16 Jy at 4.9 GHz. [At lower resolution, the 15 GHz image and 5 GHz VLBApls image (Fomalont et al. 2000b) show that more diffuse emission extending up to 10 mas to the NE

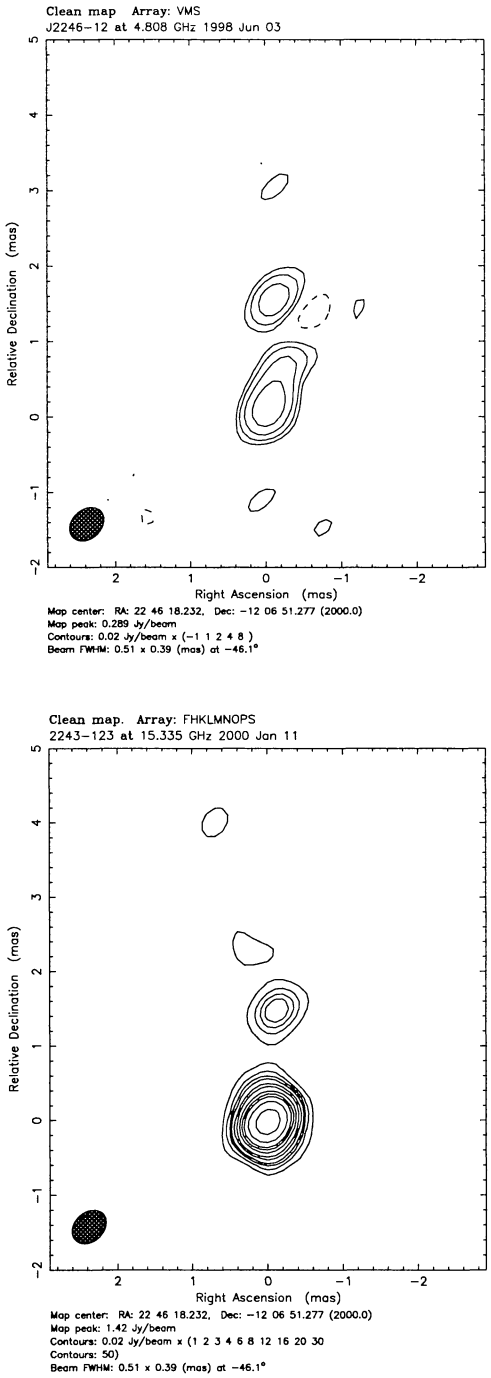

Fig. 4. Radio emission from J2246−1206 at 5 GHz and at 15 GHz: (Top) The VSOP Survey 5 GHz image at epoch 1998.43; (Bottom) The VLBA 15 GHz image at epoch 2000.03. The resolution of both images are 0.51 mas × 0.39 mas in position angle −46°1. The lowest contour level is 0.02 Jy with a peak flux density at 5 GHz of 0.289 Jy and at 15 GHz of 1.42 Jy. For the VSOP observation, the ground telescopes used were Mopra and Shanghai, the tracking stations were Usuda and Green Bank, the correlator was Penticton, and on-source time was 5.2 hr. For the VLBA observations, all ten VLBA antennas were used for an on-source time of 0.4 hr.

is also present.] Nearly half of the VSOP source list will have similar supporting 15 GHz images.

These two observations are separated by 17 months so that flux density variations and component motions may have occurred over this period. In the VLBApls observations in 1996.45, the flux density of the two components at 4.9 GHz was 1.78 Jy; in 1998.43 the flux density was 0.67 Jy, indicating a significant decrease in the flux density. A similar decrease was observed in the total flux density of the source from ATCA monitoring from 1996.5 at four frequencies (Tingay et al. in preparation). Also, component motions can be determined from comparisons amongst the various images. For the 5 GHz VSOP observations in 1998.43, the fainter component was 1.36 mas to the north. For the 15 GHz observations in 2000.03, the fainter component was 1.45 mas to the north, indicating motion away from the core.

7. Summary

The agreements made by ISAS with global observatories, with tracking stations, with correlator centers, and with a host of other supporting personnel and organizations have formed the basis for success of the VSOP Survey Program. Over two-thirds of the 289 sources in the observing sample have been observed as of 2000 July and the reduction and imaging are complete for more than half of these sources.

The preliminary results show that a large number of radio sources have significant emission on the longest HALCA baselines, corresponding to an angular size < 0.15 mas with a brightness temperature in excess of 5×10^{12} K. With the statistical completeness anticipated with the survey database, realistic tests of radio source models involving Doppler beaming, superluminal motions, and intra-day variability, can be made. A comparison of the VSOP Survey images with other high-resolution ground images and with other astronomical information will clearly aid in understanding the phenomena associated with AGN evolution. The VSOP Survey Program has demonstrated that hundreds of sources can be studied in future space missions at even higher resolution.

We gratefully acknowledge the VSOP Project, which is led by the Institute of Space and Astronautical Science in cooperation with many organizations and radio telescopes around the world.

The National Radio Astronomy Observatory is a facility of the National Science Foundation operated under cooperative agreement by Associated Universities, Inc. The Australia Telescope is funded by the Commonwealth Government for operation as a national facility by CSIRO. The Canadian S2 Space-VLBI correlator is supported by funding from the Canadian Space

Agency and the National Research Council of Canada. Part of the research was carried out at the Jet Propulsion Laboratory, California Institute of Technology under contract to NASA. The Nicolaus Copernicus University in Torun, Poland is supported by the Polish Government through the State Committee for Scientific Research under the annual grant SPUB. The Noto Observatory thanks the Italian Space Agency for financial support. The Hartebeesthoek Radio Astronomy Observatory wishes to thank the Canadian Space Agency, the Dominion Radio Observatory at Penticton and the Space Geodynamics Laboratory of the Centre for Research in Earth and Space Technology for the loan of an S2 Recording terminal. The Australia Telescope National Facility is also thanked for providing one of their Data Acquisition Systems. The Green Bank Tracking Station is operated by the National Astronomy Observatory with funding provided by NASA. The MERLIN/VLBI National Facility is operated by the University of Manchester on behalf of PPARC.

The Operations at Torun were supported by Messrs. Borkowsky, Pazderski, Jakubowicz and Kepa. For the Kalyazin operations, we thank Y. Ilyasov (Pushchino Observatory) and B. Poperechenko (Special Research Bureau of Moscow Power Engineering Institute), and the staff of the Kalyazin Observatory for providing operational and logistical support. The Hartebeesthoek Radio Astronomy Observatory thanks M. Khumalo for assistance with the HALCA observations.

References

Carlson B.R., Dewdney P.E., Burgess T.A., Casorso R.V., Petrachenko W.T., Cannon W.H. 1999, PASP 111, 1025

Fomalont E.B., Frey S., Paragi Z., Gurvits L.I., Scott W.K., Taylor A.R., Edwards P.G., Hirabayashi H. 2000b, ApJS in press

Fomalont E., Hirabayashi H., Murata Y., Kobayashi H., Inoue M., Burke B., Dewdney P., Gurvits L. et al. 2000a, in Astrophysical Phenomena Revealed by Space VLBI, ed H. Hirabayashi, P.G. Edwards, D.W. Murphy (ISAS, Sagamihara) p167

Gregory P.C., Scott W.K., Douglas K., Condon J.J. 1996, ApJS 103, 427

Griffith M.R., Wright A.E. 1993, AJ 105, 1066

Hirabayashi H. 2000, Adv. Space Res. 26, 751

Hirabayashi H., Hirosawa H., Kobayashi H., Murata Y., Asaki Y., Avruch I.M., Edwards P.G., Fomalont E.B. et al. 2000, PASJ 52, 955

Hirabayashi H., Hirosawa H., Kobayashi H., Murata Y., Edwards P.G., Fomalont E.B., Fujisawa K., Ichikawa T. et al. 1998, Science 281, 1825 and erratum 282, 1995

Johnston K.J., Fey A.L., Zacharias N., Russell J.L., Ma C., de Vegt C., Reynolds J.E., Jauncey D.J. et al. 1995, AJ 110, 880.

Kardashev N.S. 1997, Exp. Astron. 7, 329

Kellermann K.I., Vermeulen R.C., Zensus J.A., Cohen M.H. 1998, AJ 115, 1295.

Kellermann K.I., Vermeulen R.C., Zensus J.A., Cohen M.H. 2000, in Astrophysical Phenomena Revealed by Space VLBI, ed H. Hirabayashi, P.G. Edwards, D.W. Murphy (ISAS, Sagamihara) p159

Kovalev Yu.A., Kovalev Y.Y., Nizhelsky N.A. 2000, in Astrophysical Phenomena Revealed by Space VLBI, ed H. Hirabayashi, P.G. Edwards, D.W. Murphy (ISAS, Sagamihara) p193

Kühr H., Witzel A., Pauliny-Toth I.I.K., Nauber U. 1981, A&AS 45, 367

Lawrence C.R., Bennett C.L., Hewitt J.N., Langston G.I., Klotz S.E., Burke B.F., Turner K.C. 1986, ApJS 61, 105

Lovell J.E.J., Horiuchi S., Moellenbrock G., Hirabayashi H., Fomalont E., Dodson R., Dougherty S., Edwards P. et al. 2000, in Astrophysical Phenomena Revealed by Space VLBI, ed H. Hirabayashi, P.G. Edwards, D.W. Murphy (ISAS, Sagamihara) p183

Moellenbrock G.A., Fujisawa K., Preston R.A., Gurvits L.I., Dewey R.J., Hirabayashi H., Inoue M., Kameno S. et al. 1996, AJ 111, 2174

Moellenbrock G.A., Lovell J., Horiuchi S., Fomalont E., Hirabayashi H., Dodson R., Dougherty S., Edwards P. et al. 2000, in Astrophysical Phenomena Revealed by Space VLBI, ed H. Hirabayashi, P.G. Edwards, D.W. Murphy (ISAS, Sagamihara) p177

Napier P.J., Bagri D.S, Clark B.G., Rogers A.E.E., Romney J.D., Thompson A.R., Walker R.C. 1994, IEEE Proc. 82, 658

Peck A.B., Beasley A.J. 1998, in Radio Emission from Galactic and Extragalactic Compact Radio Sources, ed J.A. Zensus, G.B. Taylor, J.M. Wrobel, ASP Conf. Ser. 144, p155

Preston R.A., Morabito D.D., Williams J.G., Faulkner J., Jauncey D.L., Nicolson G.D. 1985, AJ 90, 1599

Shepherd M.C. 1997, in Astronomical Data Analysis Software and Systems VI, ed G. Hunt, H.E. Payne, ASP Conf. Ser. 125, p77

Shibata K.M., Kameno S., Inoue M., Kobayashi H. 1998, in Radio Emission from Galactic and Extragalactic Compact Radio Sources, ed J.A. Zensus, G.B. Taylor, J.M. Wrobel, ASP Conf. Ser. 144, p413

Ulvestad J.S., Linfield R.P. 1998, in Radio Emission from Galactic and Extragalactic Compact Radio Sources, ed J.A. Zensus, G.B. Taylor, J.M. Wrobel, ASP Conf. Ser. 144, p397